

Electron Reflection Coefficient at Zero Energy. I. Experiments*

H. HEIL AND J. V. HOLLWEG†

Hughes Research Laboratories, Malibu, California

(Received 19 June 1967)

The zero-energy reflection coefficient of electrons at a freshly evaporated silver surface has been measured to be $7\% \pm 1\%$. The coefficient rises linearly with $39\% \text{ eV}^{-1}$ above zero energy. In the experiments, particular care is taken that only those electrons which have actually interacted with the surface are counted; those which have been reflected by the applied field without interaction with the surface are not counted. This is accomplished by (1) use of a total-energy spectrometer, and (2) simultaneous recording of the energy spectrum and target current. Therefore, the reflection coefficient determined is essentially that for orthogonal incidence. The experimental method is critically discussed. In Sec. VI, the linear rise of reflection immediately above zero energy is attributed to atomic scattering at the surface. The reflection coefficient at zero energy can be fully explained by the patch-effect theory presented in paper II.

I. INTRODUCTION

THE reflection coefficient of slow electrons at a surface is simply measured by directing a beam of electrons toward the surface and measuring the amount of current which is returned. At primary energies below a few electron volts, no secondary electrons are created at the surface, and the true reflection coefficient of primaries is measured. At very low energies, it becomes difficult to keep the primary beam collimated and to be certain that all of the returning electrons have actually interacted with the surface (i.e., that none have returned before reaching the surface). Therefore, most of the previous measurements stopped at 1 eV or just below this value.

In order to define more precisely the term "interaction with the surface," we must refer to the various forces experienced by the primary electron as it approaches the surfaces. At distances of microns or more from the surface, only the applied electric field is effective which is retarding and is represented by plane equipotentials; the electron trajectories appear as parabolas curving away from the surface. The electric field of the crystal patches¹ with different surface potentials is felt next. This field deflects and reflects the incoming electron. Next, the image force accelerates the electron straight into the surface. Finally, the very strong forces of the atoms cause atomic scatter; the atoms scatter partly backward with the possibility of escape. We say that an electron has interacted with the surface if it has interacted with any of the last three forces which have their origin at the surface.

The reflection coefficient of slow electrons has been investigated experimentally over a period of more than 30 years; Fowler and Farnsworth² have reviewed the

older work thoroughly. We shall discuss briefly four of the more recent investigations. Fowler and Farnsworth² energy-selected a beam by a cylindrical electric field, and by means of a system of round apertures fed it into a collector containing a plane target. The electric field between collector and target is carefully zeroed, assuring that no reflected electron would be recollected. However, no provision is made for either a mechanical or a magnetic alignability of the optical system which precedes the entry to the collector and target. Therefore, at the lowest energies it cannot be determined which electrons are returned before interacting with the surface, and which are returned after such interaction. At energies above several kT , a linear increase of the reflection coefficient is observed with a slope comparable to that seen by us. Gorodetskii³ observed similar curves when he measured the reflection coefficient and the secondary-emission yield down to a primary energy of 1 eV for several surfaces. Below 1 eV the energy spectrum of the arriving beam is not known sufficiently, and in this case it is also difficult to determine how many of the returning electrons have actually interacted with the surface. Zollweg⁴ separated the arriving and returning beams and energy-analyzed the latter. Unfortunately, his analysis concerned only the axial energy at the final collector. The axial energy is not conserved along the beam because the beam is deflected in the electrostatic lenses and in the deflection field; this causes an uncertainty about the energy spectrum of the arriving beam. Therefore, it is again uncertain whether all the electrons have interacted with the surface, and it is necessary to be cautious in drawing conclusions concerning the value and behavior of the true reflection coefficient at zero energy, especially when the measurements indicate an increase at zero energy.

The work which comes closest to our measurements in the retarding regime was reported by Shelton⁵ and later by Kisliuk.⁶ Both use a close-spaced, plane-parallel

*The work reported herein was partially supported by Air Force Cambridge Research Laboratories under Contract AF 19(628)-4297.

†Hughes Doctoral Fellow, Massachusetts Institute of Technology, Cambridge, Massachusetts.

¹The effect of the patches is discussed in detail in H. Heil, following paper, Phys. Rev. 164, 887 (1967), hereafter referred to as paper II.

²H. A. Fowler and H. E. Farnsworth, Phys. Rev. 111, 103 (1958).

³D. A. Gorodetskii, Radiotekhn. i Elektron. 3, 345 (1958) [English transl.: Radio Eng. Electron. (USSR) 3, 61 (1958)].

⁴R. J. Zollweg, Surface Sci. 2, 409 (1964).

⁵H. Shelton, Phys. Rev. 107, 1553 (1957).

⁶P. Kisliuk, Phys. Rev. 122, 405 (1961).

diode consisting of a single-crystal emitter and target, a positive electrode with a small aperture between the emitter and the target, and a strong collimating magnetic field perpendicular to these three elements. The target current-voltage characteristic resembles quite accurately an ideal Maxwellian for axial energy (viz., a simple exponential change of current with retarding voltage). The slope measures the emitter temperature. At the "upper knee" the simple exponential turns sharply (within 20 mV) into saturation. The saturation current is practically constant.

Shelton is also able to measure directly the reflection coefficient at the upper knee. When the target is made more positive than the electrode with the aperture, the originally reflected current is increasingly returned to the target, and collection becomes complete. From the transition to 100% collection, he is able to derive a reflection coefficient of 6%. His conclusion that the rise to 100% is a result of the decrease of the actual reflection coefficient, and particularly that it is a result of a linear coefficient which comes out of wave-mechanical calculations of reflection off a simple potential step,⁷⁻⁹ cannot be justified. A simple return and recollection of the reflected portion of the beam in the electric field between the collector and the aperture is more plausible.

Shelton's Fig. 4 shows immediately above the retarding regime a slope of the reflection coefficient which has the same sign as that seen in the earlier work² and also by us—an increase of reflection with energy. We shall see later that this reflection coefficient is not the zero-energy coefficient R_0 , but an average coefficient R_e related to the linear slope R_1 and to R_0 as given by Eq. (10) of Sec. V. In the light of this analysis, Shelton's values read $R_e = 6\%$, $R_1 = 1\%$ eV⁻¹, $kT = 0.15$ eV, and the zero-energy coefficient $R_0 = 4.5\%$.

In this paper we describe a method for measuring the total energy spectrum of the current arriving at the surface simultaneously with that accepted at the target surface. This is accomplished with a two-lens electron-optical system, which assures orthogonal incidence. A fine, plane mesh is used as the target. Since the average reflection coefficient depends only on the ratio of the two currents, we make recordings of the target current versus the collector current. The experimental evidence, as well as the theoretical reasoning used in Sec. VI, suggest that the coefficient about zero energy consists only of a constant and a term linear in energy. The average coefficient measured throughout the retarding regime may then be decomposed into these two terms, and the true zero-energy coefficient may be deduced.

II. DESCRIPTION OF APPARATUS

Figure 1 is a scale drawing of the tube and components. The tube is housed in a glass envelope which is

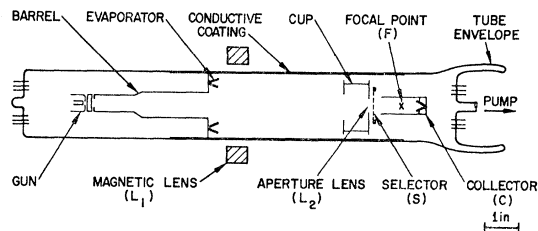


FIG. 1. View of the discharge tube which contains the electron gun, the energy spectrometer electrodes, and the evaporators.

connected to a vacuum system pumped by a vacuum pump. The entire system is bakable, and the final tube pressure is in the nTorr range. The selector consists of a mesh with 1500 openings per in. with an optical transmission of 34.2%. This mesh serves as the target. In order that the surface be well defined, silver evaporators are provided on both sides of the mesh. The evaporator on the right is mounted at the bottom of the collector C. The electron-optical elements shown from left to right in Fig. 2 are: (1) the gun, which has an oxide cathode and is the standard design used in vidicon-camera tubes; (2) the magnetic lens, mounted external to the envelope so that it can be aligned; (3) a conductive coating on the inside of the glass envelope, which ensures uniform potential through the space from the gun to the cup; (4) the cup, which consists of an aperture (on the left) which prevents scattered or stray electrons from entering the second lens, and an opening (on the right) which forms that second lens; (5) the selector; and (6) the electron collector, which collects all of the electrons which come through the mesh.

III. THE ELECTRON ENERGY SPECTROMETER AND $I_c(U_s)$ AND $I_s(U_c)$ RECORDINGS

The electron energy spectrometer is of the retarding potential type described elsewhere,¹⁰ and has been used in a number of problems which require the measurement of energy-distribution functions of electrons and ions.¹¹ Therefore, we give only a brief description here.

In Fig. 2 we can see the essential element, an electrostatic divergent aperture lens formed by the selector S and by the aperture, which is situated in front of the selector and is part of the cup. The electrons arriving from the left are in a field-free space until they reach this aperture. Two peripheral rays are shown in the figure. The divergent lens has a focal point F which is marked at the intersection of the extension of these rays with the optical axis. If the incoming convergent electron beam is focused into F, the aperture lens will cause

¹⁰ B. W. Scott and H. Heil, Air Force Scientific Report AFCRL-66-769, 1966 (unpublished); available from CFSTI, 5285 Port Royal Road, Springfield, Virginia 22151. See also H. Heil, Bull. Am. Phys. Soc. 7, 488 (1962).

¹¹ J. Y. Wada and H. Heil, IEEE J. Quantum Electron. QE-1, 327 (1965); J. Y. Wada and H. Heil, in *Proceedings of the Seventh International Conference on Ionization Phenomena in Gases, Belgrade, 1965* (Belgrade, 1966), p. 247; J. Y. Wada, R. C. Knechtli, and H. Heil, *ibid.*, p. 424.

⁷ L. A. MacColl, Phys. Rev. 56, 699 (1939).

⁸ L. A. MacColl, Bell System Tech. J. 30, 888 (1951).

⁹ P. H. Cutler and J. C. Davis, Surface Sci. 1, 194 (1964).

the rays to arrive orthogonally at the plane of the mesh. This is exactly true only for the energy-spectral portion of the incoming current which is just being returned at the mesh, or which arrives with zero kinetic energy.

The degree of collimation is limited by the following three factors: (1) the finite extent of the image which would form at the focal point F ; (2) the spherical aberrations of the aperture lens L_2 ; and (3) the potential penetration into the opening of the mesh. The first of these factors also depends on the size of the final aperture in the gun and the aberrations of the main lens, shown as L_1 in Fig. 2. To reduce the effect of these three factors, the gun aperture is made small ($50\ \mu\text{m}$ in diameter), and the image is approximately the same size. The aberrations of the aperture lens have been calculated by Heil and Wagner¹² for the special case in which the selector and aperture are coplanar and are quite small. The defects arising from the coarseness of the mesh are reduced by the use of a very fine mesh and small applied fields. Thus, with careful alignment the electron beam contains transverse velocity components which correspond to far less than $1\ kT$ of energy as they approach the mesh.

The portion of the current which passes through the mesh openings is slightly accelerated and collected by the collector. It is called I_c . The current collection must be complete, i.e., all backscattered and secondary electrons must be recollected. Figure 3 shows the extent to which this has been achieved. I_c is plotted as a function of U_s , the potential applied to the selector with reference to the gun cathode. When saturation has been reached, the constancy of I_c is better than 1%. The differentiation of the curve of I_c with respect to U_s yields the total energy spectrum $S(\epsilon)$, where ϵ is the total energy. $S(\epsilon)$ is a useful quantity for considering the energy-dependent acceptance functions in Secs. IV and V. A Maxwellian electron energy spectrum has the form $\epsilon \exp(-\epsilon/kT)$. This form is very closely approximated by the $I_c(U_s)$ recordings in our experiments.

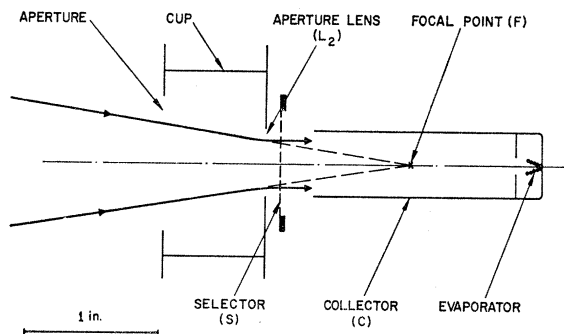


FIG. 2. Detail of energy spectrometer showing the aperture lens L_2 , the selector mesh S , and the collector assembly. The angle of approach of the two trajectories shown is exaggerated.

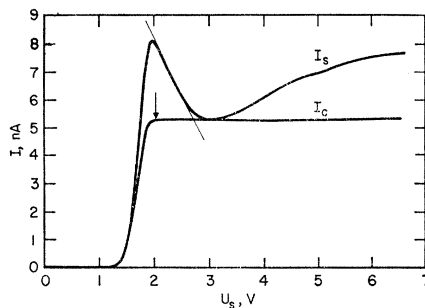


FIG. 3. Reproduction of a double recording of currents I_c (collector) and I_s (selector) versus the selector voltage U_s . (Meeting of the two curves at about 3 V is accidental in this recording.) The linear portion of I_s above 2 V indicates a slope in reflection coefficient of 39% per eV.

The second curve in Fig. 3 represents the current accepted by the selector I_s , the current arriving minus the current reflected. The electrons returning from the mesh are all released at the front surface, and the electric field about the mesh causes all of them to be returned to the gun side of the selector. Therefore, it is certain that no reflected electrons reach the collector. In the portion above the retarding regime—above about $U_s=2\text{ V}$ —the curve $I_s(U_s)$ faithfully traces the acceptance coefficient as a function of energy for the mesh surface. Initially, a linear decrease with energy is noted, which was generally observed in the earlier experiments quoted above.

We shall make use of the initial slope of the coefficient, which measures 39% eV^{-1} , in extrapolating to the zero-energy coefficient in the following section.

IV. DERIVATION OF THE ACCEPTANCE COEFFICIENT FROM $I_s(U_s)$ AND $I_c(U_s)$ IN THE RETARDING REGIME

In the retarding regime— $U_s < 2\text{ V}$ in Fig. 3—the electron-reflection coefficient of the mesh surface may be determined as follows. In the absence of reflection, the ratio of the collector current I_c to the total current is equal to the geometrical-transmission coefficient τ_0 of the mesh, which may be measured easily by optical means prior to tube assembly. If I_{s0} is the current incident on the mesh surface, then

$$\tau_0 \equiv I_c / (I_{s0} + I_c). \tag{1}$$

However, some fraction of the current I_{s0} is reflected, and only the current I_s is accepted. Thus, we may define the electron-acceptance coefficient α_e by

$$\alpha_e \equiv I_s / I_{s0}. \tag{2}$$

From (1) and (2) we find

$$\alpha_e = \frac{\tau_0 I_s}{1 - \tau_0 I_c}, \tag{3}$$

¹² H. Heil and W. G. Wagner, Rev. Sci. Instr. 35, 981 (1964).

which appears simply as the ratio of the two measurable currents, multiplied by a factor depending on the geometrical-transmission coefficient.

However, because of the nonzero energy spread, the value of α_e thus obtained represents an acceptance coefficient averaged over the energy distribution of the primary beam. Given the full energy-dependent acceptance coefficient $\alpha(\epsilon)$, we can compute the average α_e since we know the energy-distribution function from $I_c(U_s)$. The intensity of the energy spectrum $S(\epsilon)$ may be measured in A eV^{-1} and is defined such that $S(\epsilon)d\epsilon$ is the beam-current element for which the electrons have a total energy between ϵ and $\epsilon+d\epsilon$. Let us choose the reference for the voltage U_s such that the zero of U_s is the selector potential for which the slowest electron in the beam has zero kinetic energy at the mesh. In this notation the retarding regime is characterized by $U_s < 0$. The currents I_c and I_s then appear as the following integrals over the energy spectrum:

$$I_c(U_s) = \tau_0 \int_{-eU_s}^{\infty} S(\epsilon) d\epsilon, \quad U_s \leq 0 \quad (4)$$

$$I_s(U_s) = (1 - \tau_0) \int_{-eU_s}^{\infty} \alpha(\epsilon + eU_s) S(\epsilon) d\epsilon, \quad U_s \leq 0. \quad (5)$$

Here the argument $\epsilon + eU_s$ of the acceptance function α indicates the energy with which the current element $S(\epsilon)d\epsilon$ impinges at the mesh.

From a close inspection of $I_c(U_s)$ in Fig. 3, one sees that $S(\epsilon)$ is a Maxwellian of total energy, or

$$\begin{aligned} S(\epsilon) &\propto \epsilon e^{-\beta\epsilon}, & \epsilon > 0, \\ S(\epsilon) &= 0, & \epsilon < 0, \end{aligned} \quad (6)$$

where $\beta = 1/kT$. For the spectrum of Fig. 3, the beam temperature is 1060°K , or $\beta = 11 \text{ eV}^{-1}$. There are only slight deviations noticeable at the zero of energy—upper knee or slow tail—which probably indicate a nonuniform potential minimum in front of the cathode surface.

The first factor under the integral of (5), the acceptance-coefficient function $\alpha(\epsilon)$, may be described by a constant $\alpha(0) = \alpha_0$ and a linear term $\alpha_1\epsilon$ as we shall justify in Sec. VI,

$$\alpha(\epsilon + eU_s) = \alpha_0 + \alpha_1(\epsilon + eU_s). \quad (7)$$

Using (6) and (7), we can now integrate (5) and (4) and finally calculate the average acceptance coefficient α_e .

$$\alpha_e = \alpha_0 + (\alpha_1/\beta)[1 + 1/(1 - \beta eU_s)], \quad U_s < 0. \quad (8)$$

The coefficient α_e which, according to (3), may be determined for any value of U_s by the two currents I_s and I_c and by τ_0 may, according to (8), be decomposed into the two terms α_0 and α_1 , which make up the general function $\alpha(\epsilon)$ around $\epsilon = 0$. It is necessary to know the electron temperature,

The dependence of α_e on U_s is noticeable only around the upper knee, and it disappears quickly as one goes deeper into the retarding regime, where $\beta_e U_s \ll 0$ and $S(\epsilon) \propto \exp(-\beta\epsilon)$ rather than $\propto \epsilon \exp(-\beta\epsilon)$. In this regime,

$$\alpha_e = \alpha_0 + \alpha_1/\beta, \quad \beta_e U_s \ll 0, \quad (9)$$

which means α_e is a constant and hence the current ratio I_s/I_c is a constant.¹³ Because the deep retarding regime offers this simple relation, we went to a different method of recording in which I_s is recorded versus I_c . Then the sensitivity of the two current meters may be increased by as much as a factor of 100, and one can observe whether the ratio I_s/I_c remains constant as expected from Eq. (3) and (9) in the very deep retarding regime.

V. THE I_s VERSUS I_c PLOT

In Fig. 4 we show a reproduction of an $I_s(I_c)$ recording. The horizontal axis marks the collector current I_c which saturates at 5.8 nA. The selector current I_s , shown on the left axis, rises to a value between 8 and

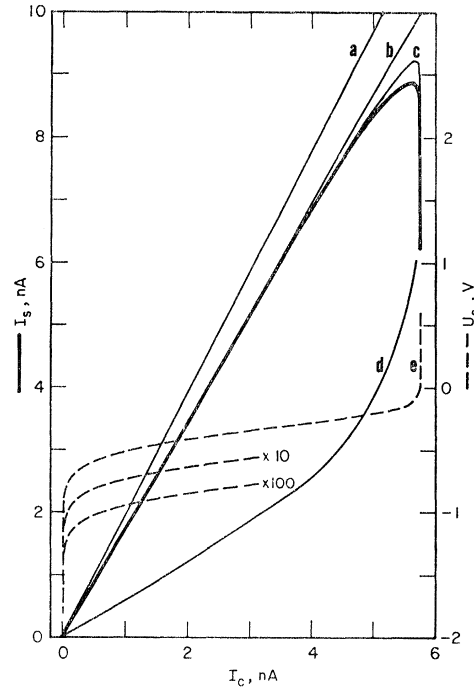


FIG. 4. Heavy solid curve, selector current I_s versus collector current I_c in the retarding regime; dashed curve e, the corresponding retarding-potential plot of retarding potential U_s versus I_c ; U_s has been chosen to be zero when the slowest electron has zero energy at the selector; a beam temperature of 1060°K is found from the fast tail, which is marked by "x10, x100." Light solid lines: (a) I_s versus I_c calculated for $\alpha = 100\%$; (b) for $\alpha = 89\%$ to match initial slope; (c) for $\alpha(\epsilon) = (93 - 39\epsilon)\%$ to match the initial slope as in (b) and the α_1 coefficient determined experimentally as shown in Fig. 3; (d) for $\alpha(\epsilon) = 1 - \exp(-\epsilon/0.19)$.

¹³ This is so not only for $\alpha(\epsilon) = \alpha_0 + \alpha_1\epsilon$, but for any function $\alpha(\epsilon)$. In general, $\alpha_e = \int_0^\infty \alpha(\epsilon) \exp(-\beta\epsilon) d\epsilon$ is a constant throughout the deep retarding regime.

9 nA and then decreases above the retarding regime. For the sake of comparison, we also show the $I_c(U_s)$ curve as a dashed line; the voltage U_s is marked on the right boundary of the figure, and one may notice the shift in reference for U_s . $U_s=0$ V is that mesh potential at which even the slowest electron is able to pass the mesh, and at which complete saturation of I_c begins.

Let us now compare the recorded $I_s(I_c)$ curve with curves which are expected if certain acceptance functions $\alpha(\epsilon)$ are assumed. Curve a of Fig. 4 is a straight line and represents the case of $\alpha=100\%$. Curve b is also a straight line and is chosen to match the initial slope of the experimental curve. It corresponds to $\alpha=89\%$. In both these cases $\alpha(\epsilon)$ is assumed to be independent of energy.

For the further cases, we refer to three $\alpha(\epsilon)$ functions, which are plotted in Fig. 5; curve A is taken from Refs. 8 and 9 and shows the reflection off potential steps of various shapes, calculated wave mechanically. In this case, $\alpha(\epsilon)$ is approximately 95% and a very slight increase on the order of 1% eV^{-1} is found from the calculation. Curve B represents the linear slope measured in Fig. 3 above the retarding-potential regime. In curve C we show a function assumed in Refs. 14 and 15 on the basis of experimental retarding-potential measurements. In this case the acceptance goes to 0 at zero energy and rises exponentially as $1-\exp(-5.2\epsilon)$.

Returning to Fig. 4, the case c represents $\alpha_0=93\%$ and $\alpha_1=39\%$ eV^{-1} . This example corresponds to case B of Fig. 5. The fourth case, marked d, is the result of a direct calculation using (4) and (5) and assuming the acceptance coefficient C in Fig. 5. This is the case where the coefficient goes to zero exponentially and is in quite obvious contradiction to the observations. In order to determine more accurately the initial portion of the $I_s(I_c)$ curve, we expanded the sensitivity of each of the two current meters by a factor of 10 and found a continuation of the same initial slope.

For further discussion, we return to the more customary notation of reflection coefficient, where $R(\epsilon)\equiv 1-\alpha(\epsilon)$, $R_0\equiv 1-\alpha_0$, $R_1\equiv -\alpha_1$, and

$$R_e = R_0 + R_1/\beta, \quad \beta_e U_s \ll 0. \quad (10)$$

A measurement at two different β values would uniquely measure both R_0 and R_1 , with both measurements made in the retarding regime. However, it is not easy experimentally to vary the electron temperature sufficiently that the value R_1 may be recognized separately. The regime immediately above the retarding regime, where $I_c(U_s)$ has just saturated, gives the correct value of R_1 . In this regime, we always find a straight stretch, although sometimes it is over only a short energy range.

¹⁴ W. B. Nottingham, Phys. Rev. **49**, 78 (1936). The experimental basis is found in A. R. Hutson, *ibid.* **98**, 889 (1955). An alternative interpretation of Hutson's experiments is suggested by G. F. Smith, *ibid.* **100**, 1115 (1955).

¹⁵ W. B. Nottingham, in *Handbuch der Physik*, edited by S. Flugge (Springer-Verlag, Berlin, 1956), Vol. 21, p. 103 ff.

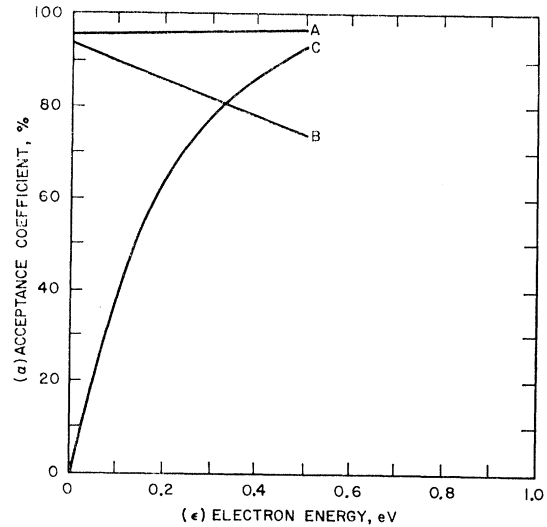


Fig. 5. Acceptance coefficient $\alpha(\epsilon)$ as a function of energy ϵ ; (A) wave-mechanical reflection off potential steps of various shapes; (B) taken from the recording shown in Fig. 3 in the high-energy range and extended to zero energy; (C) as postulated to fit early experimental data (see Ref. 14).

Taking this value for R_1 , and taking β from our energy spectrum, we find the term $R_1/\beta=3.6\%$. From this, one may see that it is generally necessary to take the slope R_1 into account in order to extrapolate accurately the zero-energy reflection coefficient R_0 from (10).

Finally, we discuss a factor which enters directly into the determination of R_0 , which caused us considerable concern when the experiments began. At both sides of the selector mesh the potential rises to more positive values; therefore, a potential penetration through the mesh opening occurs. Thus, the average potential at the plane of the selector differs from the potential at the surface of the mesh. We call this difference $\Delta\phi$. In the deep-retarding regime, where the collector current depends exponentially on the selector potential, the current ratio I_s/I_c is reduced by a factor $\exp(-\beta\Delta\phi) \approx 1-\beta\Delta\phi$. In order to keep $\Delta\phi$ to a minimum, in the final experiment we used a fine mesh with 1500 openings/in. The individual openings have a radius of 3 μm . In addition, the two electric fields were chosen as low as possible, approximately 30 V cm^{-1} total. This results in an average potential penetration of less than 2 mV, and thus the R_0 values must be further reduced by about 1%. For better accuracy, a measurement of at least two values of the sum of the electric fields and a linear extrapolation to zero field should be carried out.

VI. DISCUSSION AND SUMMARY

In the preceding sections we have shown that it is possible, in principle, to derive the reflection coefficient for electrons as a function of energy about zero energy if one measures simultaneously the total-energy spectrum of the incident beam from the collector current $I_c(U_s)$ and the current accepted at the target $I_s(U_s)$, and if one

then evaluates $R(\epsilon)$ from the integrals of (4) and (5). In practice, the evaluation is done by making use of the fact that (1) the reflection coefficient has a small linear dependence on energy of a few $\% (kT)^{-1}$, and quadratic and higher terms are negligible for at least the first $10kT$; and (2) the energy spectrum of the beam produced by the customary guns with thermally emitting cathodes is simply an exponential function of energy in the deep-retarding regime. With this knowledge, the simplified method which we used above yields, with good accuracy, a value for the combination $R_0 + R_1 kT$. For the linear coefficient R_1 , one takes the value measured above the retarding regime, beginning where I_e has reached full saturation. A perfectly linear range stretching over at least a good fraction of 1 V is always seen in this regime.

We have not seen a behavior such as the increase of the reflection coefficient to 100% at zero energy. The recent observations⁴ where such an increase is suggested are presumably the result of insufficient distinction between returning electrons which have interacted with the surface and those which have been returned in the applied electric field without interaction with the surface.

It is apparent that the assumptions underlying the simple wave-mechanical calculations of the reflection off a potential step cannot be realized in an actual experiment and the predicted slight *decrease* ($R_1 < 0$) and the zero-energy value R_0 itself have not been, and cannot be seen, on real surfaces. We believe one always observes the much larger, linear *increase* ($R_1 > 0$) which comes about by the following process. Because of the image force, the slow electron is attracted into the surface, impacts with an energy of several eV, and is backscattered by the atoms of the surface layer or by adsorbed atoms. For escape, the differential scatter cross section in the backward direction is important. It should be constant within some range of angles around 180° . If this is so, the probability for escape of electrons rises linearly with energy, causing the linear increase in electron reflection which is customarily observed. This is the process described by Becker and Brattain.¹⁶ The

¹⁶ J. A. Becker and W. H. Brattain, Phys. Rev. **45**, 698 (1934). A quantitative formulation of this process by H. Heil [Bull. Am. Phys. Soc. **6**, 359 (1961); **7**, 327 (1962)] has led to a determination of the electron affinity of aluminum oxide from recordings such as that shown in this paper. Analyzed in this manner, the curve $I_e(U_e)$ of Fig. 3 indicates qualitatively that about 40% of the primaries backscatter upon first impact and that the scatter centers are situated at a position with a potential 2 V more positive

positive slope of the reflection coefficient always dominates the much smaller, wave-mechanical one which is not realized because the calculations neglect completely electron scattering during the entry of the electron wave into the material.

In our experiments, even though the primary electrons impinging on the target are well collimated, the incidence is orthogonal only to the extent that the mesh surface is parallel to the plane of the mesh. In addition, the use of a fine mesh as the target represents a severe limitation in the choice of target material. However, we have prepared a "mesh" by drilling an array of holes of $30\text{-}\mu\text{m}$ diameter spaced by $250\text{ }\mu\text{m}$; the drilling is done by spark erosion. Thus, a surface can be made of which less than 2% is disturbed by openings, and certainly more than 95% is orthogonal to the electron trajectories. This preparation makes feasible the use of single-crystal targets, which would eliminate patches entirely. If adsorbed layers are avoided, and a good low-energy electron-diffraction pattern shows a well-ordered surface, the scatter at the surface may be sufficiently eliminated and the wave-mechanically-calculated zero-energy reflection coefficient may be approached.

The extreme collimation of the electron beam at the mesh is essential not only to provide orthogonal incidence to the target surface, but mainly to assure that the interception of the electron flow by the mesh actually is exactly as indicated by the geometrical-transmission coefficient τ_0 . Electrons which do not arrive orthogonally to the plane of the mesh experience an enhanced reflection due to the small periodic potential variations above the mesh which result from the potential penetrations into the mesh openings. This type of reflection is not a property of the surface and it would falsify the measurements. The extreme collimation and the smallness of the potential penetrations assure the absence of this electrostatic reflection. Reflection in such periodic electric fields is treated in the subsequent paper.

In Paper II, we shall study by computer experiment to what extent the electric field of the patches at the silver surface causes electron reflection. The analysis will show the surprising result that independent of patch amplitude, patch size, and patch-distribution function, the zero-energy reflection coefficient is approximately 7%.

than the vacuum level. The scatter centers are probably an adsorbed layer which formed during the silver evaporation when the pressure rose to some 10^{-7} Torr and which did not desorb at the final pressure of several nTorr at room temperature.